



# Reevaluation of the phospholipid composition in membranes of adult human lenses by $^{31}\text{P}$ NMR and MALDI MS

Rosendo Estrada<sup>a</sup>, Andres Puppato<sup>a</sup>, Douglas Borchman<sup>b</sup>, M. Cecilia Yappert<sup>a,\*</sup>

<sup>a</sup> Department of Chemistry, University of Louisville, Louisville, KY 40292, USA

<sup>b</sup> Department of Ophthalmology and Visual Sciences, University of Louisville, Louisville, KY 40292, USA

## ARTICLE INFO

### Article history:

Received 27 January 2009

Received in revised form 15 September 2009

Accepted 9 November 2009

Available online 17 November 2009

### Keywords:

Human lens membrane

Phospholipid

$^{31}\text{P}$  NMR spectroscopy

Temperature coefficient

MALDI MS

## ABSTRACT

The phospholipid composition of adult human lens membranes differs dramatically from that of any other mammalian membrane. Due to minimal cell turnover, cells in the nucleus of the human lens may be considered as the longest lived cells in our body. This work reassesses previous assignments of phospholipid  $^{31}\text{P}$  NMR resonances in adult human lenses. The new assignments are based not only on chemical shifts but also on temperature coefficients. By addition of known phospholipids and examination by matrix-assisted laser desorption/ionization mass spectrometry, several misassigned resonances have been corrected. The revised composition reveals the possible presence of ceramide-1-phosphate and dihydroceramide-1-phosphate. Among glycerophospholipids, the most abundant one does not correspond to phosphatidylglycerol but may be due to the lysoform of alkyl-acyl analogs of phosphatidylethanolamine. Besides sphingophospholipids, adult human lens membranes contain significant amounts of ether (1-O-alkyl) glycerophospholipids and their corresponding lysoforms.

© 2009 Elsevier B.V. All rights reserved.

## 1. Introduction

The ocular lens offers an exceptional case for the study of aging. With minimal cell turnover, the lens provides a layer of viable epithelial cells (epithelium) as well as layers of cells at various levels of differentiation and senescence [1]. Among mammalian lenses, those from humans are of particular interest because of our long lifespan. Indeed, fiber cells found in the center of the nucleus of an adult human lens are as old as the individual. The phospholipid (PL) analysis of a primary line of fetal epithelial human cells [2] revealed markedly different composition from that of nuclear adult lenses [3,4]. Adult human lenses exhibit uniquely high contents of sphingolipids (SLs) and cholesterol [4–7]. The unusual nature of the most abundant PL component was recognized in 1991 when Merchant et al. in their influential report indicated that “the uncharacterized phospholipids do not correspond to any phospholipid commonly associated with mammalian membrane systems” [8]. After establishing the identity of this PL as dihydrosphingomyelin (DHSM) [9,10], our group has investigated regional and age-dependent trends in the PL composition of human and non-human mammalian lenses. The preferential depletion of glycerophospholipids (GPLs) in older fibers and consequent enrichment of SLs [11,12] were among the most notable age-related trends. However, the contribution of the resonance at  $\delta=0.5$  ppm, originally assigned to phosphatidylglycerol (PG), increased with age. We have been puzzled by the relative increase

in the content of this diacylglycerol-PL as the relative amounts of all others decrease with age.

Concerned with the possibility of misassignment(s) of resonances in previous analyses of human lens membranes, the correction or confirmation in the assignment of each of the resonances labeled with “?” in Fig. 1 has been pursued. By taking into account the chemical shifts and temperature coefficients of the various resonances and with the use of matrix-assisted laser desorption/ionization (MALDI) mass spectrometry (MS), this work reevaluates the unusual PL composition of adult human lens membranes and explains some of the trends that were perceived previously as inconsistent.

The temperature dependence of PL resonances has been used to minimize spectral interferences in  $^{31}\text{P}$  NMR spectral studies of PLs carried out by our research group [2,4,11,13–18] and others [19,20]. For example, an increase in temperature from 25 °C to 40 °C allowed us to resolve the band corresponding to DHSM from that originally attributed to phosphatidylethanolamine plasmalogen (PEp) [4]. Such studies also revealed a downfield shift for the resonance at  $\delta\sim 0.5$  ppm (at 25 °C), as the temperature was increased. These observations prompted the evaluation of the temperature coefficients ( $\Delta\delta/\Delta T$ ) for PLs found in most common mammalian membranes [21]. With the use of these coefficients, the identity of misassigned or unidentified resonances in the  $^{31}\text{P}$  NMR spectrum of human lens membranes has been pursued. The results show that the PLs that remain in adult human lenses are of high chemical and structural stability and point to the importance of sphingolipids and glycerol-PLs in which the *sn*-1 chain is linked to the glycerol backbone with an ether linkage (1-O-alkyl). These PLs will be referred to as ether PLs

\* Corresponding author. Tel.: +1 502 852 7061; fax: +1 502 852 8149.

E-mail address: [mcypappert@louisville.edu](mailto:mcypappert@louisville.edu) (M.C. Yappert).

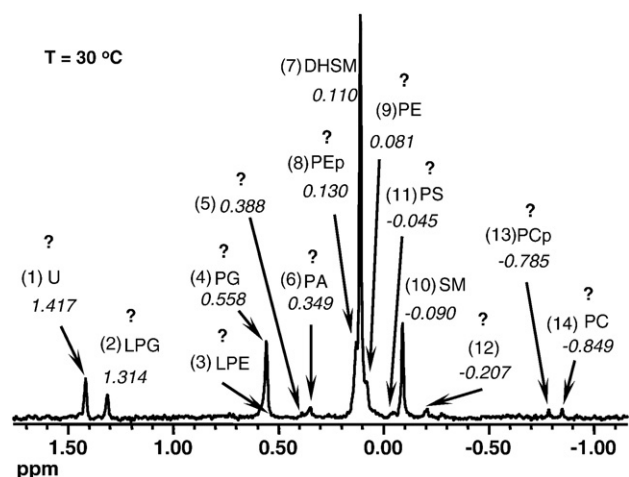


**Fig. 1.**  $^{31}\text{P}$  NMR spectrum at 30 °C of PLs extracted from human lenses. The peaks are labeled as reported previously by Merchant et al. (see Ref. [5]): Uncharacterized resonance (U), lysophosphatidylglycerol (LPG), lysophosphatidylethanolamine (LPE), phosphatidylglycerol (PG), phosphatidic acid (PA), phosphatidylethanolamine plasmalogen (PEp), phosphatidylethanolamine (PE), phosphatidylserine (PS), sphingomyelin (SM), phosphatidylcholine plasmalogen (PCp), phosphatidylcholine (PC). The resonance corresponding to dihydrosphingomyelin (DHSM) was assigned previously as an unknown signal. Chemical shifts were referenced to internal SMs ( $\delta = -0.09$  ppm). The question marks point to resonances whose assignments are readdressed in this investigation.

whereas those linked via an ether vinyl linkage (1-*O*-alk-1'-enyl) shall be referred to as plasmalogens in the rest of this report.

## 2. Materials and methods

### 2.1. Chemicals and reagents

Human lenses were obtained from the Kentucky Lions Eye Bank (Louisville, KY). All donors, protocols and procedures were approved by the Institutional Review Board at University of Louisville. All procedures were in accord with the Declaration of Helsinki. Lysophosphatidylethanolamine plasmalogen from bovine brain (LPEp) and *D*-erythro-sphingosine-1-phosphate (Sps1P) were purchased from Matreya (Pleasant Gap, PA). 3-*sn*-Phosphatidylethanolamine (PE) from bovine brain (10 mg/ml in chloroform) containing 60% 3-*sn*-phosphatidylethanolamine plasmalogen (PEp), 1,2-diacyl-*sn*-glycero-3-phospho-L-serine (PS) from bovine brain, sphingomyelin (SM) from bovine brain, phospholipase D (PLD) from *Streptomyces chromofuscus* (7010 units/mg of solid), methanol, chloroform, chloroform-*d*, platinum (IV) oxide ( $\text{PtO}_2$ ), NaCl, 2-amino-2-(hydroxymethyl)-1,3-propanediol (Tris buffer) and sodium dodecyl sulfate (SDS) were obtained from Sigma (St. Louis, MO).  $\text{CaCl}_2 \cdot 6\text{H}_2\text{O}$ , cesium chloride (CsCl), *para*-nitroaniline (PNA), and ethylenediaminetetraacetic acid (EDTA) were purchased from Aldrich Chemical (Milwaukee, WI) and Fisher Scientific (Fair Lawn, NJ), respectively. Absolute ethanol was obtained from AAPER Alcohol and Chemical (Shelbyville, KY).

Lysophosphatidylethanolamine (1-*O*-alkyl) ether (LPEe) and phosphatidylethanolamine ether (PEe) were prepared by hydrogenation of LPEp and PEp, respectively. DHSM was generated from SM. The hydrogenation procedure was similar to that reported previously [13,21]. Briefly, the PLs were dissolved in ethanol (95%)/methanol (90:10) to obtain a final concentration of 3.0 mg/ml. Methanol was added first to facilitate dissolution of the PLs.  $\text{PtO}_2$  (10% of the weight of PLs) was added as the catalyst. The sample was immersed in a temperature-controlled ultrasonic bath at 40 °C and the catalyst (10%  $\text{PtO}_2$  of the weight of PLs) was then added. The vial containing the sample was covered with a plastic stopper and hydrogen was bubbled through a needle (25G5/8 or 30G1/2) immersed in the solution. The solution was sonicated in a temperature-controlled ultrasonic bath at

40–45 °C for 3 h.  $\text{PtO}_2$  was pelleted by centrifugation. The solution containing the PLs was analyzed by  $^{31}\text{P}$  NMR and/or MALDI-TOF MS.

Ceramide-1-phosphate (Cer1P) and dihydroceramide-1-phosphate (DHCer1P) were generated by hydrolysis with PLD of SM and DHSM from bovine brain. The reaction of PLs with PLD was carried out with a protocol similar to that reported earlier [21]. Briefly, 22 mg of PLs were suspended in the following solutions that were added sequentially: 0.6 ml of 0.1 M Tris buffer (pH 8.0), 0.3 ml of 50 mM SDS and 4 ml of  $\text{H}_2\text{O}$ . Then, the following solutions were added: 27  $\mu\text{l}$  of 17.9% ethanol in water, 0.6 ml of 0.5 M  $\text{CaCl}_2$ , 0.4 ml of  $\text{H}_2\text{O}$  and 0.2 ml of PLD (20 units/ml) from *S. chromofuscus*. The mixture was homogenized and incubated at 30 °C with occasional swirling during the reaction. The reaction was terminated by adding two parts of ice-cold chloroform/methanol (3:1) to 1 part of the solution with the PLs. The organic phase was separated from the aqueous phase for further analysis.

### 2.2. Extraction of lipids from human lenses

Lipids from 14 human lenses of different ages (16 to 46, average ~34 years old) were extracted with 50 ml of methanol [22]. As indicated in Ref. [22], this monophasic extraction protocol reduces the loss of PLs observed when biphasic solvents are used to extract lens lipids. The tissue was fragmented and then homogenized with a glass-stirring rod. The sample was immersed in a temperature-controlled ultrasonic bath (Model 8890 ultrasonic cleaner, Cole-Palmer Instruments, Vernon Hills, IL, USA) for 15 min at 40 °C. After 30 min of centrifugation, the solution containing the lipids was removed from the pellet. A portion of the solvent was evaporated with the use of a rotary evaporator at 30 °C to obtain a final volume of 12 ml.

### 2.3. Analysis of PLs by $^{31}\text{P}$ NMR spectroscopy

Two milliliters of the extract of lipids from human lenses were used for analysis by  $^{31}\text{P}$  NMR spectroscopy. After removal of the solvent with a flow of nitrogen gas, the lipids were redissolved in 500  $\mu\text{l}$  of chloroform-*d* and the solution was transferred to an NMR tube. Because a significant amount of the solvent was evaporated during the transfer of the solution, more chloroform-*d* was added to the NMR tube to adjust the volume to 500  $\mu\text{l}$ . Then, 250  $\mu\text{l}$  of methanol/0.2M Cs-EDTA (4:1) reagent [23] were added and the solution was homogenized with the use of a temperature-controlled ultrasonic bath at 40 °C for 10 min. The NMR tubes were carefully sealed to minimize the evaporation of the solvent.  $^{31}\text{P}$  NMR spectral traces were recorded on a Varian Inova-500 spectrometer. The parameters to perform the acquisitions were similar to those described previously [21]. Briefly, a spectral width of 2024.7 Hz (sweep width  $\delta = 10$  ppm), 60° pulse, 4000 data points, 1.0 s delay time, 0.711 s acquisition time and proton decoupling (WALTZ) at 500.16 MHz were used. A line broadening of 3.0 Hz and phase correction were used to process the spectra. The samples were spun at 18 rps and heated at different temperatures (10–50 °C). Before each spectral acquisition, the samples were allowed to reach thermal equilibrium at each given temperature for 15 min. Temperature coefficients were calculated from the spectral data obtained between 15 and 45 °C. Chemical shifts were referenced to internal SMs ( $\delta = -0.09$  ppm). Process and integration of spectral bands were performed with Mestrec NMR software (Mestrelab Research, Santiago de Compostela, Coruña, Spain). Only bands with signal-to-noise greater than 10 were selected as resonances corresponding to PLs.

### 2.4. Analysis of PLs by MALDI MS

Positive- and negative-ion mass spectra were obtained in the reflector mode by using a Voyager Biospectrometry DE workstation (Applied Biosystems, Foster City, CA). All spectral acquisition

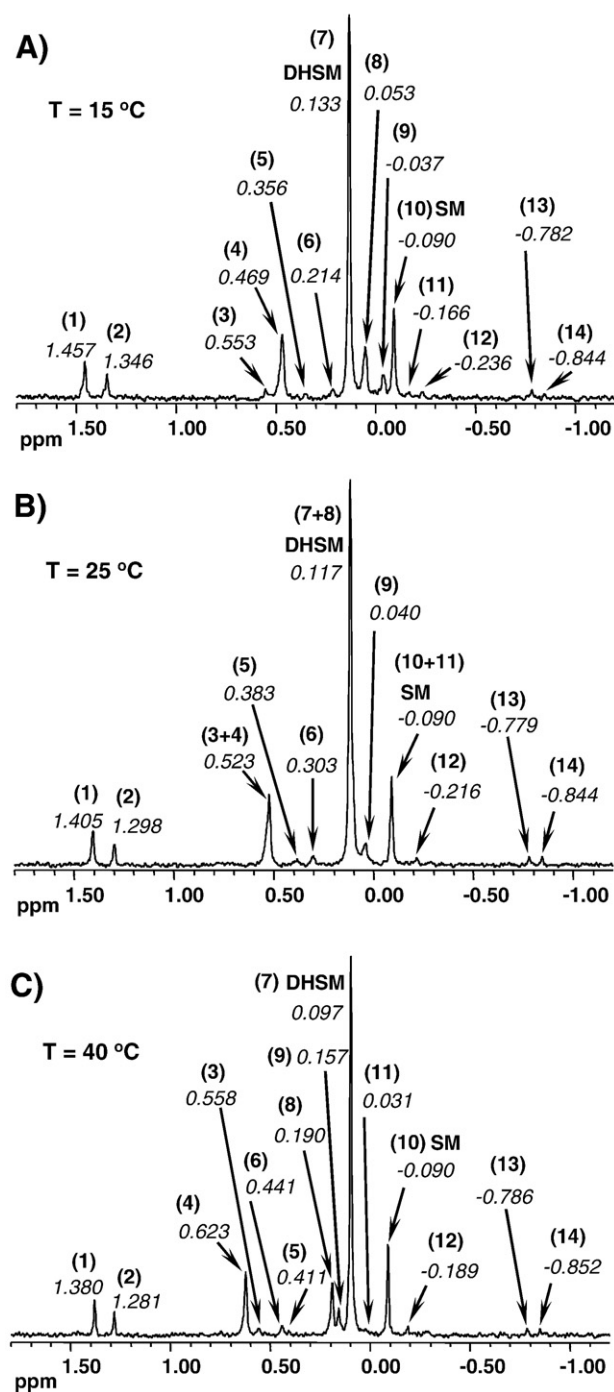


**Fig. 2.**  $^{31}\text{P}$  NMR spectra of PLs extracted from human lenses at different temperatures. Chemical shifts were referenced to internal SMs ( $\delta = -0.090$  ppm). These spectral data were used in the evaluation of the temperature coefficients listed in Table 1.

conditions and other details were similar to those reported earlier [11,14,24]. In all other experiments, 0.15 M PNA prepared in chloroform/methanol (2:1) was used as the matrix, as reported previously [2,13,14]. For the analysis in the positive mode, CsCl crystals were added to the matrix solution or to the sample to minimize spectral complexity [2,13,14].

On a 400-spot ( $20 \times 20$ ) hydrophobic plate, the lipid extract ( $0.3 \mu\text{l}$ ) was spotted first, followed by the addition of  $0.3 \mu\text{l}$  of the matrix solution. The samples were left to crystallize at room temperature. All spectra were calibrated by using a two-point mass calibration procedure. To calibrate the spectra obtained in the positive mode, a preliminary mass calibration was carried out by adding two synthetic

PLs of known masses, PA(28:0) and PG(36:0), to the lipid extract with CsCl. The peaks of  $[\text{PA}(28:0) + \text{H} + 2\text{Cs}]^+$  ( $m/z = 857.21$ ) and  $[\text{PG}(36:0) + 2\text{Cs}]^+$  ( $m/z = 1043.38$ ) were used to calibrate the positive-ion spectra. In addition to PA(28:0) and PG(36:0), CL from bovine heart was added to the sample to calibrate the negative-ion spectra. The ions corresponding to  $[\text{PA}(28:0) + \text{H}]^-$  ( $m/z = 591.40$ ),  $[\text{PG}(36:0)]^-$  ( $m/z = 777.56$ ) and  $[\text{CL}(72:8) + \text{H}]^-$  ( $m/z = 1447.96$ ) were selected to perform the calibration. The identification of PL-related peaks was carried out as reported earlier [14,24]. However, the maximum mass tolerance,  $\Delta(m/z)$ , was set at 0.03. After the masses and identities of the lipids were determined, lipids present in the lens extracts were used to perform the mass calibration. In the positive-ion mass spectra,  $\text{Cs}^+$  ( $m/z = 132.91$ ) and  $[\text{SM}(24:1) + \text{Cs}]^+$  ( $m/z = 945.58$ ) were used to calibrate the spectra.

### 3. Results

The effect of temperature on the chemical shift of PL resonances associated with lipids extracted from human lenses is illustrated in Fig. 2. When the temperature was increased from  $15^\circ\text{C}$  to  $40^\circ\text{C}$  (Fig. 2C), the chemical shift of peaks 1 and 2 shifted upfield and peaks 4, 5, 6, 8, 9, 11 and 12 shifted downfield. On the other hand, the chemical shift of peaks 3, 13 and 14 did not change significantly with temperature. As expected, peak 7—corresponding to DHSM—shifted slightly upfield with temperature. At  $15^\circ\text{C}$  (Fig. 2A) and  $40^\circ\text{C}$  (Fig. 2C), all PL resonances were resolved. However, the resonances of some PLs, such as those corresponding to peaks 3 and 4, 7 and 8, and 10 and 11 overlapped at  $25^\circ\text{C}$  (Fig. 2C). Peaks 7 and 8 were totally overlapped when the temperature was between  $32^\circ\text{C}$  and  $36^\circ\text{C}$  (spectra not shown).

#### 3.1. Preliminary assignment of PL resonances

From the temperature dependence of the PL resonances observed in the human lens lipid extract, the temperature coefficients were calculated (see Table 1) for each of the peaks observed in Fig. 2. Then, the chemical shifts at  $25^\circ\text{C}$  and temperature coefficients were compared with those reported previously [21] to assign each resonance. The proposed assignments are listed in column 4 of Table 1. SM was used as an internal reference because its assignment, as well as that for the DHSM resonance, was confirmed previously by our research group [9,10]. Moreover, SM was used as an internal reference in our previous work [21] to study the chemical shift dependence of various PLs with temperature.

**Table 1**

Chemical shift ( $\delta$ ) at  $25^\circ\text{C}$  and temperature coefficient ( $\Delta\delta/\Delta T$ ) of PLs extracted from human lenses.

Peak no.	$\delta \pm \text{S.D. (ppm)}$ at $25^\circ\text{C}$	$\Delta\delta/\Delta T \pm \text{S.D., } 10^{-3}$ (ppm/ $^\circ\text{C}$ )	Proposed assignment
1	$1.396 \pm 0.059$	$-4.2 \pm 0.7$	DHCer1P
2	$1.291 \pm 0.061$	$-3.7 \pm 0.8$	Cer1P
3	0.550	$-0.1$	PGe
4	$0.524 \pm 0.007$	$5.9 \pm 0.8$	LPEe
5	0.382	2.3	Not assigned
6	$0.290 \pm 0.019$	$8.8 \pm 0.6$	LPSe
7	<b><math>0.116 \pm 0.002</math></b>	<b><math>-1.6 \pm 0.2</math></b>	<b>DHSM</b>
8	$0.119 \pm 0.007$	$5.5 \pm 0.6$	PEe
9	$0.030 \pm 0.016$	$7.9 \pm 0.5$	PSe
10	<b><math>-0.090</math></b>	<b>Reference</b>	<b>SM</b>
11	$-0.086$	–	PS
12	$-0.215 \pm 0.005$	$1.9 \pm 0.2$	LPCE
13	$-0.779 \pm 0.001$	$-0.2 \pm 0.3$	PCe
14	$-0.843 \pm 0.003$	$-0.2 \pm 0.2$	PC or/and PCp

The chemical shifts and temperature coefficients were measured for each of the 14 resonances shown in Fig. 1. By comparison of the values with those obtained for known PLs (see Ref. [21]), the new assignments were made. DHSM and SM are in bold font because the accuracy of these assignments has been demonstrated before (see Ref. [10]). The abbreviations used in this table are listed in List of abbreviations.



### 3.1.1. Assignment of peaks 1 and 2

Based on their chemical shifts, resonances 1 and 2 in Fig. 2A could be due to DHCer1P, and/or Cer1P, and/or Sps1P, and/or DHSps1P and/or lysophosphatidylglycerol (LPG). However, the temperature coefficients of peaks 1 ( $-4.2 \times 10^{-3}$  ppm/°C) and 2 ( $-3.9 \times 10^{-3}$  ppm/°C; see Table 1) corresponded only to those of DHCer1P ( $-4.1 \times 10^{-3}$  ppm/°C) and Cer1P ( $-3.9 \times 10^{-3}$  ppm/°C) reported earlier [21]. These coefficients are very distinct from those corresponding to the other possible PLs. For example, the temperature coefficient previously reported for LPG was  $2.0 \times 10^{-3}$  ppm/°C [21], quite different in sign and magnitude to those for peaks 1 and 2. The chemical shift difference ( $\Delta\delta \sim 0.11$  ppm) between these peaks was maintained at all temperatures and the same difference was observed for these SPLs ( $\Delta\delta \sim 0.11$  ppm) in previous studies with known PLs [21].

### 3.1.2. Assignment of peak 3

Peak 3 could be due to PG and/or the lysoforms of ethanolamine-containing GPLs, such as lysophosphatidylethanolamine (LPE), LPE ether (LPEe), and LPE plasmalogen (LPEp). However, because the chemical shift of this peak did not change significantly with temperature, ethanolamine-containing GPLs were discarded as they exhibit temperature coefficients between  $6.5 \times 10^{-3}$  ppm/°C and  $6.8 \times 10^{-3}$  ppm/°C.

The temperature coefficient of peak 3 ( $-0.1 \times 10^{-3}$  ppm/°C) was significantly close to that of PG ( $-0.2 \times 10^{-3}$  ppm/°C) determined earlier [21], but the  $\delta$  of peak 3 ( $\delta = 0.550$  ppm) was 0.085 ppm higher (downfield) than that of PG ( $\delta = 0.465 \pm 0.014$  ppm) [21]. This suggested that peak 3 could be due to a PL ether with a glycerol head group, phosphatidylglycerol ether (PGe) or phosphatidylglycerol plasmalogen (PGp) because the temperature coefficient matches that of PG. Based on the trends previously observed in PLs with ethanolamine head group, the 0.085-ppm downfield shift of peak 3 with respect to that of PG resonance also suggests that this peak may be possibly due to PGe and not to PGp. For example, the resonances of PEE and PEP are  $\sim 0.094$  ppm and  $\sim 0.040$  ppm, respectively, downfield from that of PE.

### 3.1.3. Assignment of peak 4

Based on its chemical shift, resonance 4 could be assigned to PG and/or the lysoform of ethanolamine-containing GPLs. However, PG was excluded because the temperature coefficient of peak 4 ( $5.9 \times 10^{-3}$  ppm/°C) was different from that reported for PG ( $-0.2 \times 10^{-3}$  ppm/°C). Instead, the temperature coefficients of ethanolamine-containing GPLs reported earlier [21] were significantly close ( $\sim 6.6 \times 10^{-3}$  ppm/°C) to that of peak 4. From this observation as well as others to be discussed later, peak 4 was assigned to LPEe.

### 3.1.4. Assignment of peak 5

Peak 5 could not be assigned because we have not found any species with a temperature coefficient of  $2.3 \times 10^{-3}$  ppm/°C and with a chemical shift close to 0.383 ppm.

### 3.1.5. Assignment of peak 6

The chemical shifts of cardiolipin (CL;  $\delta = 0.168$  ppm), PA ( $\delta = 0.180$  ppm), and phosphatidic acid plasmalogen (PAP;  $\delta = 0.223$  ppm) [21] were the closest to that of peak 6 ( $\delta = 0.290 \pm 0.019$  ppm). However, peak 6 could not be due to any of those species because the temperature coefficients of CL ( $0.5 \times 10^{-3}$  ppm/°C), PA ( $-3.1 \times 10^{-3}$  ppm/°C) and PAP ( $-3.1 \times 10^{-3}$  ppm/°C) are significantly different from that of the peak 6 ( $8.8 \times 10^{-3}$  ppm/°C).

The temperature coefficient of peak 6 matches that of lysophosphatidylserine (LPS;  $8.7 \times 10^{-3}$  ppm) reported previously [21], but its chemical shift was 0.172 ppm higher than that of LPS ( $\delta = 0.118 \pm 0.054$  ppm) observed in previous studies [21]. With the same reasoning presented above for the assignment of peak 3, peak 6 may be due to alkyl lysophosphatidylserine ether (LPSe).

### 3.1.6. Assignment of peak 7

As expected, the temperature coefficient ( $-1.6 \times 10^{-3}$  ppm/°C) of peak 7 and chemical shifts at all temperatures correspond to those of DHSM resonance.

### 3.1.7. Assignment of peak 8

The  $\Delta\delta/\Delta T$  ( $5.5 \times 10^{-3}$  ppm/°C) of peak 8 matches those reported for GPLs with an ethanolamine head group ( $\sim 5.6 \times 10^{-3}$  ppm/°C) [21]. By considering the chemical shifts, this peak could be either assigned to PEE or PEP, but its chemical shift was closer to that of PEE. In addition, the chemical shift difference between peak 4 (assigned to LPEe) and this peak (8) was  $0.421 \pm 0.005$  ppm at 25 °C. In Ref. [21],  $\delta(\text{LPEe}) - \delta(\text{PEe}) = 0.417 \pm 0.005$  ppm. Therefore, peak 8 was tentatively assigned to PEE.

### 3.1.8. Assignment of peak 9

The chemical shift of peak 9 ( $\delta = 0.030 \pm 0.016$  ppm) was between those reported earlier for PEP ( $\delta = 0.058 \pm 0.007$  ppm) and PE ( $\delta = 0.018 \pm 0.007$  ppm). Its temperature coefficient ( $7.9 \times 10^{-3}$  ppm/°C), however, was significantly higher than those observed for resonances due to PE-related PLs ( $\sim 5.6 \times 10^{-3}$  ppm/°C). Therefore, peak 9 could not be assigned to either PEP or PE.

The highest temperature coefficient reported for known PLs corresponds to PS ( $8.0 \times 10^{-3}$  ppm/°C) but the  $\delta$  for PS ( $\delta = -0.148 \pm 0.038$  ppm) previously reported [21] is 0.178 ppm lower than that of peak 9 ( $0.030 \pm 0.016$  ppm). As mentioned in the assignment of peak 3, this difference in chemical shift could be expected between the ether (alkyl, acyl) and the diacyl PLs. Therefore, peak 9 was tentatively assigned to phosphatidylserine ether (PSe).

Another consideration that would support this assignment is the chemical shift difference between peak 9 and peak 6, which has been assigned to LPSe. This difference was measured to be  $0.260 \pm 0.006$  ppm. For PS and its corresponding lysoform, LPS, the difference in chemical shifts is higher,  $0.300 \pm 0.011$  ppm, as reported in Ref. [21]. This suggests that peaks 6 and 9 cannot be related to LPS and PS, respectively. At this time, the chemical shift difference between resonances due to LPSe and PSe is not known. If trends similar to those observed for ethanolamine-containing PLs were to apply, the smallest chemical shift difference would be expected for the lysoform (LPSe) and its parent PS ether (PSe). For ethanolamine-containing PLs, the chemical shift difference between resonances due to LPEe and PEE was 0.417 ppm, whereas that for LPE and PE was higher (0.439 ppm) and reached its largest value for peaks associated with plasmalogen species, LPEp and PEP (0.496 ppm). Further studies with known PLs are necessary to confirm the assignment of peak 9.

### 3.1.9. Assignment of peak 11

The temperature coefficient of peak 11 was not calculated because this peak did not appear in some spectra due to its low intensity. At 25 °C and at 45 °C, this peak was overwhelmed by the peaks corresponding to SM (at 25 °C) or DHSM (at 45 °C). Peak 11 was tentatively assigned to PS because its chemical shift was significantly close to that of PS found previously.

### 3.1.10. Assignment of peak 12

The temperature coefficient of peak 12 ( $1.9 \times 10^{-3}$  ppm/°C) was significantly close to that reported for lysophosphatidylcholine (LPC;  $2.2 \times 10^{-3}$  ppm/°C) [21], but its chemical shift ( $\delta = -0.215$  ppm) was 0.076 ppm higher (downfield) than that of LPC ( $\delta = -0.291$  ppm). Because the chemical shift of peak 4 is higher than that of LPC and the temperature coefficient is close to that of LPC, this peak could be due to ether form of LPC (LPCE). Lysophosphatidylcholine plasmalogen (LPCp) was considered to be an unlikely possibility because, just as for PC and PCp, the resonances for LPC and LPCp cannot be resolved in the solvent system used in this study.

The chemical shift difference between peaks 12 and 14 (PC and/or PCp) was 0.628 ppm. This value is 0.095 ppm higher than the difference reported previously ( $\delta(\text{LPC}) - \delta(\text{PC and/or PCp}) = 0.533$  ppm) [21] and further suggests that peak 12 could not be due to LPC.

### 3.1.11. Assignment of peaks 13 and 14

The chemical shifts of peaks 13 and 14 match those of phosphatidylcholine ether (PCE) and PC and/or PCp listed in Ref. [21]. Moreover, the temperature coefficients of peak 13 ( $-0.2 \times 10^{-3}$  ppm/°C) and peak 14 ( $-0.2 \times 10^{-3}$  ppm/°C) are significantly close to those listed for PCE ( $-0.3 \times 10^{-3}$  ppm/°C) and PCp ( $-0.3 \times 10^{-3}$  ppm/°C) [21]. In addition, at all temperatures, the chemical shift differences between peaks 13 and 14 ( $\Delta\delta = \sim 0.060$  ppm) were the same as that reported between PCE and PC or PCp ( $\Delta\delta = \sim 0.060$  ppm) [21].

### 3.2. Supporting information on the identity of some resonances by addition of known PLs and MALDI MS

To check the plausibility of the assignments of some of the resonances, the sample was spiked sequentially with Cer1P, LPEe, PEE, PE, PS and Sps1P. Fig. 3 shows the  $^{31}\text{P}$  NMR spectra of extracted PLs from human lens membranes before (Fig. 3A) and after the addition of these PLs (Fig. 3B and C). The thicker arrows in Fig. 3B and C indicate the known PLs added to the sample. After the addition of each PL, the spectral traces were obtained at different temperatures (spectra not shown) to remove spectral overlap and determine the temperature coefficients.

It is important to mention that the addition of these species into the sample produced changes in the chemical shifts of the resonances initially present. For example, comparing the chemical shifts of PLs in Fig. 3B with respect to Fig. 3A, the resonances corresponding to PCE and PC (and/or PCp), PCE, PSe, DHSM, PLSe, Cer1P and DHCer1P shifted upfield to different extents. With respect to Fig. 3B, the addition of Sps1P shifted downfield the peaks corresponding to DHCer1P, Cer1P, LPSe, PS, LPCe, PCE and PC/PCp, the resonances of LPEe, PEE and PCE moved upfield and the peak corresponding DHSM did not change significantly (see Fig. 3C). The resonances of PE and PSe overlapped.

These changes in chemical shift were expected, because previous studies have shown that various factors, such as type of counterions [23,25], proportion of lipids present in the sample [20,26], concentration of PLs [27], pH [20,28], solvent composition [20,25,27–29], and temperature [2,4,11,13,15,19–21,27,28] can affect the chemical shift of PL resonances. In this work, the slight changes in chemical shifts could be due to changes in the total concentration and composition of the lipids and also to small changes in pH.

#### 3.2.1. Supporting information on the identities of peaks 1 and 2

The identity of peak 2 as Cer1P was supported by the results obtained after the addition of Cer1P. Sps1P was also added because the resonance of this SPL as well as that of DHSps1P appear significantly close to that of peaks 1 and 2. DHSps1P was not added because the resonance of this species overlapped with that of Sps1P at all temperatures used previously.

After spiking the sample with Cer1P (Fig. 3B) the intensity of the peak tentatively assigned to Cer1P increased by a factor of 5. Changes in temperature did not produce splitting of this peak and the chemical shift differences between the peaks corresponding to DHCer1P minus that of Cer1P ( $\sim 0.11$  ppm) was maintained at all temperatures, as observed previously with known PLs [21]. These observations lend further evidence to the assignments of peaks 1 and 2 as DHCer1P and Cer1P, respectively.

Because the chemical shift for Sps1P is within the range of peaks 1 and 2, we spiked the sample with Sps1P. As shown in Fig. 3C, the Sps1P resonance appeared at  $\delta = 1.342$  ppm—between those of DHCer1P (1.392 ppm) and Cer1P (1.284 ppm). When the temperature

was increased, the peak corresponding to Sps1P shifted downfield and those related to DHCer1P and Cer1P shifted upfield. These results indicate that neither resonance 1 or 2 is due to Sps1P. Furthermore, DHSps1P can be also ruled out because, just as for Sps1P, its temperature coefficient is positive [21].

The possible presence of DHCer1P and Cer1P was checked using MALDI MS. Fig. 4A shows the negative-ion mass spectrum acquired for the human lens extract with the use of PNA as the matrix [13]. The peaks with highest intensity were observed at  $m/z = 618.49$  and 728.60, followed by those at  $m/z = 616.46$  and 726.58. These peaks

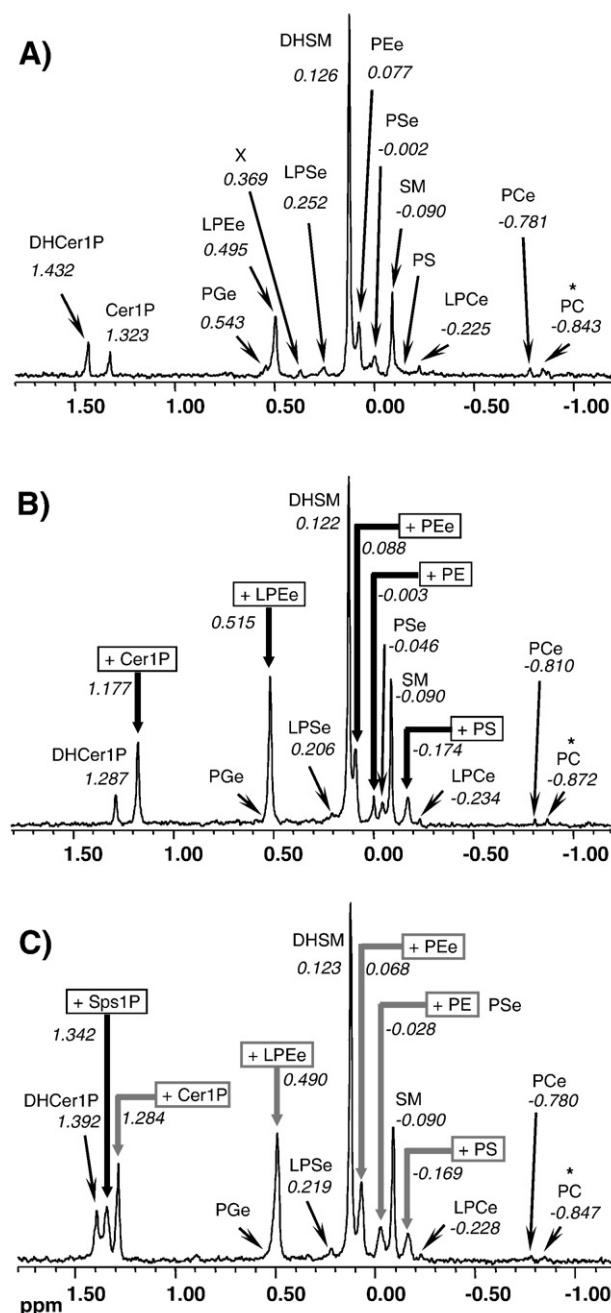


**Fig. 3.**  $^{31}\text{P}$  NMR spectra of PLs extracted from human lenses at 20 °C before and after addition of known PLs. The added PLs are shown in boxes. (A) Sample before being spiked. (B) Sample spiked sequentially with Cer1P, PE and PEE, LPEe and PS. (C) Sample in (B) was spiked with Sps1P. Chemical shifts were referenced to internal SM ( $\delta = -0.090$  ppm). \*This peak may be also due to PCp because the resonance of this PL overlaps with that of PC.

were tentatively assigned to PEE(28:1) ( $m/z=618.45$ ), PEP(28:1) ( $m/z=616.43$ ), PEE(36:2) ( $m/z=728.56$ ) and PEP(36:2) ( $m/z=726.54$ ) because their  $m/z$  values were within 0.06 Da of the theoretical values calculated for those species. Recent reports based on electrospray ionization (ESI) MS have also assigned the peak at  $m/z=728.6$  to PEE(36:2) [30–32]. Upon MS/MS analysis Deeley et al. obtained fragments that supported their assignment.

We noticed, however, that the difference between that of the peaks at  $m/z=728.60$  and  $m/z=618.49$  and that between the peaks at  $m/z=726.58$  and  $m/z=616.46$  was 110.11 Da. This difference in  $m/z$  values matches that observed in positive-ion mass spectra (Fig. 4B) between the two most abundant SPLs, DHSM(24:1) ( $m/z=947.60$ ) and DHSM(16:0) ( $m/z=837.49$ ); and SM(24:1) ( $m/z=945.58$ ) and SM(16:0) ( $m/z=835.47$ ) was 110.11 Da. This observation led us to

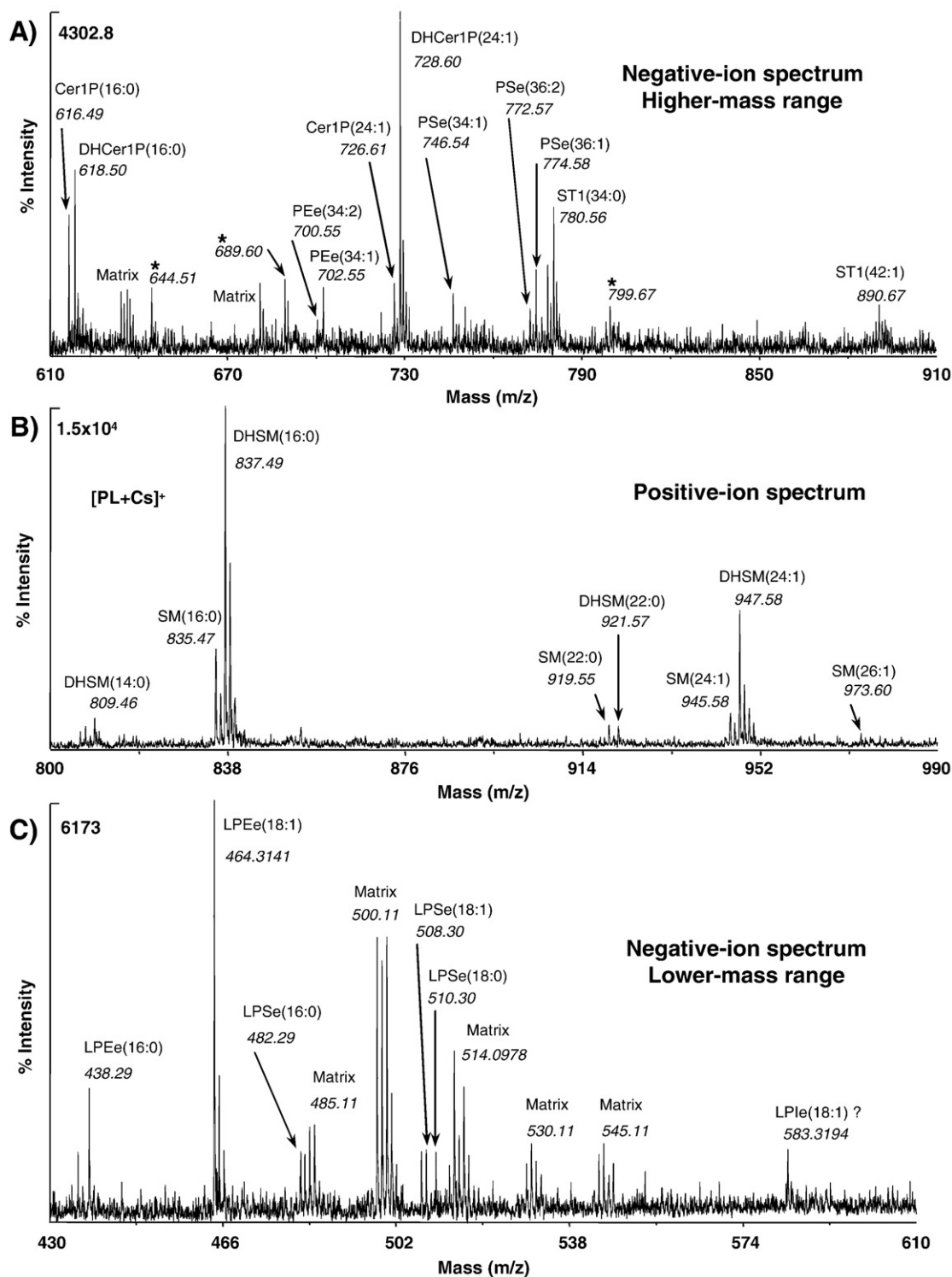


**Fig. 4.** MALDI spectra collected for the human lens extract to support the new assignments for the  $^{31}\text{P}$  NMR resonances. (A) Negative-ion spectrum. Two sulfatides (ST1) were also detected. (B) Positive-ion spectrum showing the Cs adducts of SM and DHSM. (C) The lower mass range shows the possible presence of LPEs with 16:0 and 18:1 alkyl chains and of LPSse. \*Possible fragments of SM and DHSM.

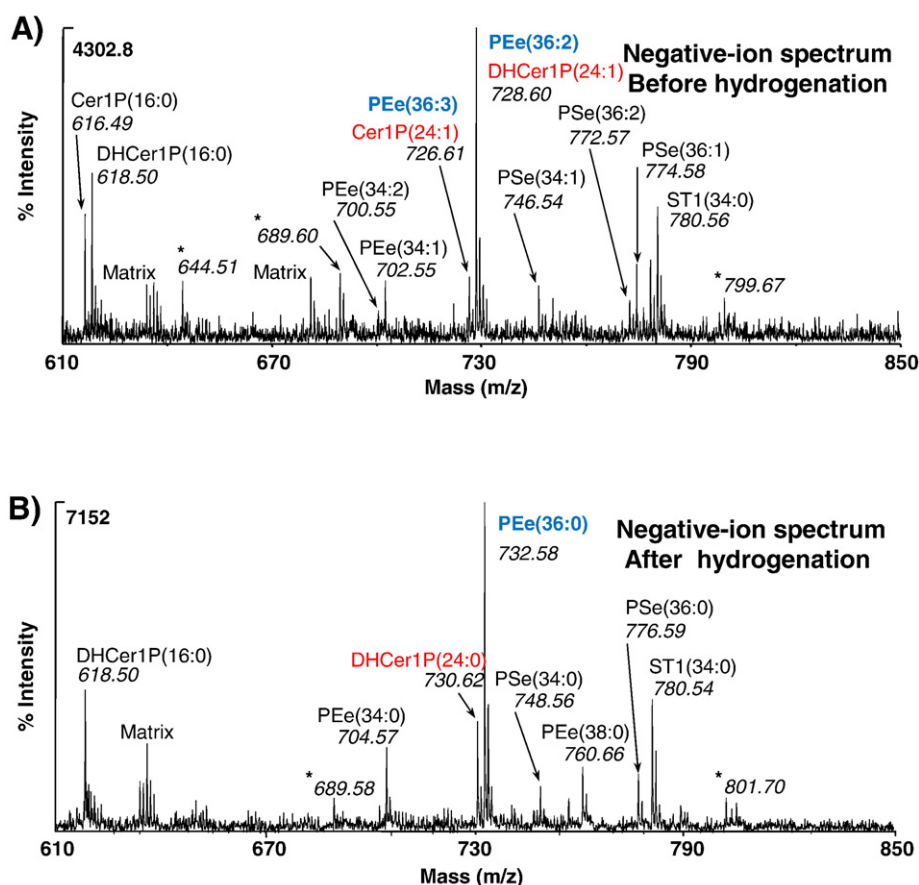


Fig. 5. MALDI negative-ion spectra collected (A) before and (B) after 3 h of hydrogenation. \*Possible fragments of SM and DHSM.

suggest the possible presence of ceramide-containing PLs with the same hydrophobic tails as those of DHSMs and SMs. Based on this consideration, the peaks at  $m/z=618.49$  and  $728.60$  could also be related to DHCer1P(16:0) and DHCer1P(24:1), respectively, whereas those at  $m/z=616.47$  and  $726.58$  could correspond to Cer1P(16:0) and Cer1P(24:1), respectively.

To further explore this possibility, the sample was hydrogenated. If the peak at  $m/z=728.60$  corresponded solely to PEE(36:2), an increase in four atomic mass units (amu) should be observed. If the peak was due to DHCer(24:1), the increase would be 2 amu. Fig. 5B shows the spectrum obtained after hydrogenation. Indeed, and consistent with the identification reported by Deeley et al., most of the peak originally at  $728.6$  shifted to  $732.6$  (see Fig. 5). There was, however, a smaller peak at  $730.6$ . Although this peak could be the saturated DHCer(24:0), it could also be related to partially hydrogenated PEE(36:1) and further analysis is needed to verify its identity. Attempts to perform post-source decay (PSD) did not allow the complete separation and thus adequate selection of the desired peak.

### 3.2.2. Supporting information on the identity of peak 4

After the addition of LPEe, the intensity of peak 4 increased by a factor of 2 (Fig. 3B and C). After increasing or decreasing the temperature, the peak did not split and the temperature coefficient matched that of LPEe. The presence of LPEes was also confirmed by MALDI MS. Fig. 4C shows the negative-ion mass spectrum for the range below 600 Da in which the peaks at  $m/z=438.29$  and  $464.31$  are assigned to LPEe(16:0) and LPEe(18:1), respectively. Although relative to other PLs, PE-related species are more difficult to detect by MALDI MS, [33–35] the relative contribution of peak 4 in the NMR spectrum shown in Fig. 1 is relatively high and enables sensitive MS detection, as evidenced in Fig. 4C.

### 3.2.3. Supporting information on the identity of peak 8

To check the identity of peak 8, the sample was spiked first with PEE and then with PE. When PEE was added (Fig. 3B and C), the intensity of peak 8 increased by a factor of 1.6. On the other hand, the addition of PE generated a new peak at  $\delta=-0.003$  ppm, between those of PEE and PSe at  $20^\circ\text{C}$  (Fig. 3B). As expected, the peak corresponding to PEE was  $\sim 0.094$  ppm downfield from that of PE at all temperatures. The  $\Delta\delta/\Delta T$  values of PEE and PE obtained in this experiment match those reported previously for PEE and PE [21].

In agreement with the results reported by Deeley et al., the peaks at  $m/z=700.55$  and  $702.55$  in Fig. 4A can be assigned to PEE(34:2) and PEE(34:1) [32].

### 3.2.4. Supporting information on the identities of peaks 9 and 11

The addition of PS led to a significant enhancement in the resonance corresponding to peak 11, thus supporting the initial assignment of this band to PS. Because the temperature coefficient of peak 9 is that of a PL with a serine head group and the  $\delta(\text{peak 11}) - \delta(\text{PS}) > 0.1$  ppm, peak 9 may be due to PSe. The  $\delta(\text{PSe}) - \delta(\text{PS})$  has not been determined previously, but it is known from observation in other PLs, such as those with ethanolamine head group, that the chemical shift difference between the ether PL and the diacyl PL is  $\sim 0.1$  ppm. The mass spectral data in Fig. 4A reveals the presence of PSe (36:1) as the most abundant PSe species. ESI-MS studies reported that PSe made up about 4% of the total human PLs [30].

## 4. Discussion

Fig. 6 includes in italics resonance assignments reported previously [8,9,10] and in bold font those corrected in this work. The study



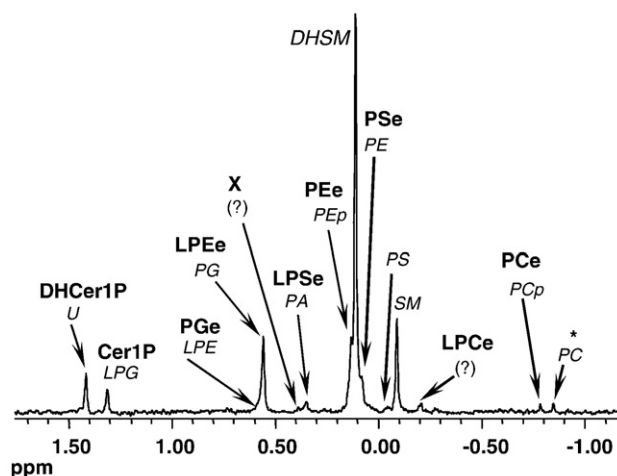


**Fig. 6.**  $^{31}\text{P}$  NMR spectrum at 30 °C of PLs extracted from human lenses. Previous assignments are indicated in *italics* and those corrected in this work appear in **bold** letters. Chemical shifts were referenced to internal SMs ( $\delta = -0.09$  ppm). \*This peak may be also due to PCp because the resonance of this PL overlaps with that of PC. The question mark (?) denotes peaks that had not been reported or assigned before and correspond to peaks 5 and 12 in Fig. 1.

of temperature coefficients in known PLs in their diacyl, ether and plasmalogen forms, sphingolipids and their metabolites provided fundamental information for the correction or corroboration of assignments in the  $^{31}\text{P}$  NMR spectrum of PLs present in human lens membranes. For example, the resonance originally assigned to PG exhibited a temperature coefficient very similar to that observed for PLs with an ethanolamine head group but very different from that of the PG resonance that hardly changes with temperature. This observation and the chemical shift differences measured between known diacyl, alkyl-acyl, alkenyl-acyl PLs, and their corresponding lyso analogs led to the assignment of this resonance (peak 4 in Fig. 1) to LPEe. Furthermore, the corresponding parent PL, PEE, was also found to be present in human lens membranes [30–32]. The relative abundance of PEE decreases with age and this PL is absent in cataractous tissue [18].

It is quite coincidental that the mass of a PEE species, PEE(36:2) at  $m/z = 728.559$  reported recently [30–32] is 0.037 amu different from the value for DHCer(24:1)1P. The hydrogenation study presented herein suggests that it is likely that both lipids may be present in adult human lenses. Given the age-dependent increase in lipid order [36], it would be interesting to see if the levels of PEE(36:2) decrease with age. Interestingly, the plasmalogen analogs, LPEp and PEP, were absent. With these corrected assignments, a new trend can be discerned in the age-dependent changes previously reported for human lenses [3–8]: diacyl and plasmalogen PLs are preferentially depleted and lead to the relative enrichment of ether glycerol-PLs and their corresponding lysoforms. These changes are particularly clear for PE-related species and suggest that the assignments of peaks 3, 6, 9 and 12 as PGE, LPSe, PSe and LPCe are reasonable.

The possible depletion of plasmalogen in older and cataractous lens membranes is consistent with reports that indicate their high reactivity due to the presence of a vinyl-ether bond. Indeed, plasmalogen are more reactive than other PLs and are believed to act as scavengers to protect other PLs from oxidative reaction [37]. Since human lens cells are not regenerated and the synthesis of PLs only takes place in the outer fibers, it is reasonable to expect either the absence or total depletion of plasmalogen-related PLs in older cells. Moreover, the *cis* configuration of the  $\alpha$ ,  $\beta$ -unsaturated ether linkage in plasmalogen puts a rigid 30° bend in the alkenyl chain that interferes with efficient packing [38]. Therefore, as the diacyl and plasmalogen PLs undergo enzymatic and/or oxidative catabolism, the remaining alkyl-acyl-PLs and their lysoforms, without the *cis* double

bond, are chemically stable and can pack tightly to form a highly ordered membrane. Older and cataractous human lens membranes exhibit unusually high levels of hydrocarbon chain order [36,39,40].

As reported previously, the relative levels of both DHSM and SM also increase with age but DHSM is the most abundant in human lenses. Consistent with the paragraphs above, DHSM without a *trans* double bond between carbons 4 and 5 of the sphingoid backbone can bind more tightly to neighboring PLs and cholesterol [12].

The possible presence of Cer1P and DHCer1P is a new finding that deserves further attention and confirmation. Metabolic studies in other cells revealed that Cer1P can be formed by enzymatic removal of the choline moiety of SM or by cleavage of the phosphocholine group in SM or the sugar head group of gangliosides followed by phosphorylation via ceramide kinase [41]. Because the possible presence of these species in human lens membranes had not been recognized before, their metabolism and functional roles remain to be investigated. In our previous report, the resonances for both Cer1P and DHCer1P were absent in membranes from mixed and mature posterior subcapsular human cataracts. Compared to clear human lenses, the contributions of these two SPLs were 50% lower in nuclear cataractous lenses [18]. It is also interesting to note that our group reported the absence of these two PLs in cholesterol-enriched domains isolated from human lenses [4].

Whereas the peak assigned to Cer1P (previously believed to be related LPG) was observed in other mammals [11], the resonance proposed to be due to DHCer1P was not detected. As the data in Ref. [11] indicate, the content of Cer1P appears to increase with the age of the animal and in older fibers within the same lens. These observations further suggest that Cer1P is a possible catabolite of SM and its relative content is enhanced with age.

Despite the high spectral resolution provided by the solvent system introduced by Meneses and Glonek [23], the correct assignment of the resonances of PLs extracted from human lens membranes has been challenging, as several of these PLs are not commonly found in other membranes and/or their resonances overlap with those of other PLs. With the use of temperature coefficients and sequential addition of known PLs, this investigation has corrected the assignment of several resonances. Although further confirmation by independent methods of several of the new assignments remains to be addressed and is underway in our laboratory, the new identities of these PLs appear to be quite reasonable and they reconcile previous inconsistencies between the PL composition reported in 1991 from  $^{31}\text{P}$  NMR results [8] and that published nearly four decades ago by Broekhuysse from TLC separations [42].

From the biological viewpoint, much remains to be learned. The PL composition of fetal human lens epithelial cells differs dramatically [2] from those at older ages. Therefore, it is possible that the metabolites of depleted PLs may participate in pathways that lead to lens development and aging. Understanding human lens metabolism could lead to new ways of preventing or treating lens malformations and opacification.

#### List of abbreviations

##### Glycerophospholipids (GPLs)

CL	cardiolipin
PA	phosphatidic acid (2 acyl chains)
PAP	phosphatidic acid plasmalogen (alkenyl-acyl chains)
PC	phosphatidylcholine (2 acyl chains)
PCE	phosphatidylcholine ether (alkyl-acyl chains)
PCp	phosphatidylcholine plasmalogen (alkenyl-acyl chains)
PE	phosphatidylethanolamine (2 acyl chains)
PEe	phosphatidylethanolamine ether (alkyl-acyl chains)
PEp	phosphatidylethanolamine plasmalogen (alkenyl-acy chains)
PG	phosphatidylglycerol (2 acyl chains)



PGe	phosphatidylglycerol ether (alkyl–acyl chains)
PGp	phosphatidylglycerol plasmalogen (alkenyl–acyl chains)
PS	phosphatidylserine (2 acyl chains)
PSe	phosphatidylserine ether (alkyl–acyl chains)
PSp	phosphatidylserine plasmalogen (alkenyl–acyl chains)

Note: An “L” preceding the PL abbreviation indicates the “lyso-form” with the *sn*-2 chain removed.

#### Sphingophospholipids (SPLs)

Cer1P	ceramide-1-phosphate
DHCer1P	dihydroceramide-1-phosphate
DHSM	dihydrosphingomyelin
DHSps1P	dihydrosphingosine-1-phosphate
SM	sphingomyelin
Sps1P	sphingosine-1-phosphate

#### References

- [1] N.A.P. Brown, A.J. Bron, *Lens Disorders: Clinical Manual of Cataract Diagnosis*, Butterworth-Heinemann Ltd, Oxford, 1996.
- [2] R. Estrada, D. Borchman, J. Reddan, A. Hitt, M.C. Yappert, In vitro and in situ tracking of choline-phospholipid biogenesis by MALDI TOF-MS, *Anal. Chem.* 78 (2006) 1174–1180.
- [3] D. Borchman, W.C. Byrdwell, M.C. Yappert, Regional and age-dependent differences in the phospholipid composition of human lens membranes, *Investig. Ophthalmol. Vis. Sci.* 35 (1994) 3938–3942.
- [4] M. Rujoi, J.L. Jin, D. Borchman, D.X. Tang, M.C. Yappert, Isolation and lipid characterization of cholesterol-enriched fractions in cortical and nuclear human lens fibers, *Investig. Ophthalmol. Vis. Sci.* 44 (2003) 1634–1642.
- [5] P.S. Zelenka, *Lens Lipids*, *Curr. Eye Res.* 3 (1984) 1337–1359.
- [6] R.M. Broekhuysse, *Membrane lipids and proteins in ageing lens and cataract*, in: Ciba Foundation Symposium (Ed.), The human lens in relation to cataract, 19, Elsevier, Amsterdam, 1973, pp. 135–149.
- [7] G.L. Felman, Human ocular lipids: their analysis and distribution, *Surv. Ophthalmol.* 19 (1967) 207–243.
- [8] T.E. Merchant, J.H. Lass, P. Meneses, J.V. Greiner, T. Glonek, Human crystalline lens phospholipid analysis with age, *Investig. Ophthalmol. Vis. Sci.* 32 (1991) 549–555.
- [9] S.R. Ferguson, D. Borchman, M.C. Yappert, Confirmation of the identity of the major phospholipid in human lens membranes, *Investig. Ophthalmol. Vis. Sci.* 37 (1996) 1703–1706.
- [10] W.C. Byrdwell, D. Borchman, R.A. Porter, K.G. Taylor, M.C. Yappert, Separation and characterization of the unknown phospholipid in human lens membranes, *Investig. Ophthalmol. Vis. Sci.* 35 (1994) 4333–4343.
- [11] M.C. Yappert, M. Rujoi, D. Borchman, I. Vorobyov, R. Estrada, Glycero- versus sphingo-phospholipids: correlations with human and non-human mammalian lens growth, *Exp. Eye Res.* 76 (2003) 725–734.
- [12] M.C. Yappert, D. Borchman, Sphingolipids in human lens membranes: an update on their composition and possible biological implications, *Chem. Phys. Lipids* 129 (2004) 1–20.
- [13] R. Estrada, M.C. Yappert, Regional phospholipid analysis of porcine lens membranes by matrix-assisted laser desorption/ionization time-of-flight mass spectrometry, *J. Mass Spectrom.* 39 (2004) 1531–1540.
- [14] R. Estrada, M.C. Yappert, Alternative approaches for the detection of various phospholipid classes by matrix-assisted laser desorption/ionization time-of-flight mass spectrometry, *J. Mass Spectrom.* 39 (2004) 412–422.
- [15] A. Puppato, D.B. Dupre, N. Stolowich, C. Yappert, Effect of temperature and pH on P-31 nuclear magnetic resonances of phospholipids in cholate micelles, *Chem. Phys. Lipids* 150 (2007) 176–185.
- [16] L. Huang, M.C. Yappert, J.J. Miller, D. Borchman, Thyroxine ameliorates oxidative stress by inducing lipid compositional changes in human lens epithelial cells, *Investig. Ophthalmol. Vis. Sci.* 48 (2007) 3698–3704.
- [17] L. Huang, R. Estrada, M.C. Yappert, D. Borchman, Oxidation-induced changes in human lens epithelial cells—I. Phospholipids, *Free Radic. Biol. Med.* 41 (2006) 1425–1432.
- [18] L. Huang, V. Grami, Y. Marrero, D.X. Tang, M.C. Yappert, V. Rasi, D. Borchman, Human lens phospholipid changes with age and cataract, *Investig. Ophthalmol. Vis. Sci.* 46 (2005) 1682–1689.
- [19] J.M. Pearce, R.A. Komoroski, Analysis of phospholipid molecular species in brain by  $^{31}\text{P}$  NMR spectroscopy, *Magn. Reson. Med.* 44 (2000) 215–223.
- [20] N. Sotirhos, B. Herslof, L. Kenne, Quantitative analysis of phospholipids by  $^{31}\text{P}$ -NMR, *J. Lipid Res.* 27 (1986) 386–392.
- [21] R. Estrada, N. Stolowich, M.C. Yappert, Influence of temperature on  $^{31}\text{P}$  NMR chemical shifts of phospholipids and their metabolites in: I. Chloroform-methanol–water, *Anal. Biochem.* 380 (2008) 41–50.
- [22] W.C. Byrdwell, H. Sato, A.K. Schwarz, D. Borchman, M.C. Yappert, D.X. Tang, P-31NMR, quantification and monophasic solvent purification of human and bovine lens phospholipids, *Lipids* 37 (2002) 1087–1092.
- [23] P. Meneses, T. Glonek, High resolution  $^{31}\text{P}$  NMR of extracted phospholipids, *J. Lipid Res.* 29 (1988) 679–689.
- [24] M. Rujoi, R. Estrada, M.C. Yappert, In situ MALDI-TOF MS regional analysis of neutral phospholipids in lens tissue, *Anal. Chem.* 76 (2004) 1657–1663.
- [25] T.O. Henderson, T. Glonek, T.C. Myers, Phosphorus-31 nuclear magnetic resonance spectroscopy of phospholipids, *Biochemistry* 13 (1974) 623–628.
- [26] N. Culeddu, M. Bosco, R. Toffanin, P. Pollesello,  $^{31}\text{P}$  NMR analysis of phospholipids in crude extracts from different sources: improved efficiency of the solvent system, *Magn. Reson. Chem.* 36 (1998) 907–912.
- [27] H.T. Edzes, T. Teerlink, M.S. Vanderknaap, J. Valk, Analysis of phospholipids in brain tissue by  $^{31}\text{P}$  NMR at different compositions of the solvent system chloroform-methanol–water, *Magn. Reson. Med.* 26 (1992) 46–59.
- [28] M. Bosco, N. Culeddu, R. Toffanin, P. Pollesello, Organic solvent systems for  $^{31}\text{P}$  nuclear magnetic resonance analysis of lecithin phospholipids: applications to two-dimensional gradient-enhanced  $^1\text{H}$ -detected heteronuclear multiple quantum coherence experiment, *Anal. Biochem.* 245 (1997) 38–47.
- [29] M. Branca, N. Culeddu, M. Fruiani, M.V. Serra,  $^{31}\text{P}$  Nuclear magnetic resonance analysis of phospholipids in a ternary homogeneous system, *Anal. Biochem.* 232 (1995) 1–6.
- [30] J.M. Deeley, T.W. Mitchell, X.J. Wei, J. Korth, J.R. Nealon, S.J. Blanksby, R.J.W. Truscott, Human lens lipids differ markedly from those of commonly used experimental animals, *Biochim. Biophys. Acta Mol. Cell Biol. Lipids* 1781 (2008) 288–298.
- [31] M.C. Thomas, T.W. Mitchell, D.G. Harman, J.M. Deeley, J.R. Nealon, S.J. Blanksby, Ozone-induced dissociation: elucidation of double bond position within mass-selected lipid ions, *Anal. Chem.* 80 (2008) 303–311.
- [32] J.M. Deeley, M.C. Thomas, R.J.W. Truscott, T.W. Mitchell, S.J. Blanksby, Identification of abundant alkyl ether glycerophospholipids in the human lens by tandem mass spectrometry techniques, *Anal. Chem.* 81 (2009) 1920–1930.
- [33] J. Schiller, S. Hammerschmidt, H. Wirtz, J. Arnhold, K. Arnold, Lipid analysis of bronchoalveolar lavage fluid (BAL) by MALDI-TOF mass spectrometry and P-31 NMR spectroscopy, *Chem. Phys. Lipids* 112 (2001) 67–79.
- [34] M. Petkovic, J. Muller, M. Muller, J. Schiller, K. Arnold, J. Arnhold, Application of matrix-assisted laser desorption/ionization time-of-flight mass spectrometry for monitoring the digestion of phosphatidylcholine by pancreatic phospholipase  $A_2$ , *Anal. Biochem.* 308 (2002) 61–70.
- [35] M.C. Thomas, T.W. Mitchell, S.J. Blanksby, A comparison of the gas phase acidities of phospholipid head groups: experimental and computational studies, *J. Am. Soc. Mass Spectrom.* 16 (2005) 926–939.
- [36] D. Borchman, Y. Ozaki, O.P. Lamba, W.C. Byrdwell, M.C. Yappert, Age and regional structural characterization of lipid hydrocarbon chains from human lenses by infrared, and near-infrared Raman spectroscopies, *Biospectroscopy* 2 (1996) 113–123.
- [37] P. Brites, H.R. Waterham, R.J.A. Wanders, Functions and biosynthesis of plasmalogens in health and disease, *Biochim. Biophys. Acta Mol. Cell Biol. Lipids* 1636 (2004) 219–231.
- [38] D. Voet, J.G. Voet, *Biochemistry*, John Wiley & Sons, New York, 1995.
- [39] D. Borchman, O.P. Lamba, M.C. Yappert, Structural characterization of lipid-membranes from clear and cataractous human lenses, *Exp. Eye Res.* 57 (1993) 199–208.
- [40] D. Borchman, M.C. Yappert, P. Herrell, Structural characterization of human lens membrane lipid by infrared-spectroscopy, *Investig. Ophthalmol. Vis. Sci.* 32 (1991) 2404–2416.
- [41] L. Riboni, R. Bassi, V. Anelli, P. Viani, Metabolic formation of ceramide-1-phosphate in cerebellar granule cells: evidence for the phosphorylation of ceramide by different metabolic pathways, *Neurochem. Res.* 27 (2002) 711–716.
- [42] R.M. Broekhuysse, Phospholipids in tissues of the eye. III. Composition and metabolism of phospholipids in human lens in relation to age and cataract formation, *Biochim. Biophys. Acta* 187 (1969) 354–365.